A Kinetic Analysis of Superoxide Adduct Formation in the Presence of Typical Scavengers

Keiichi MITSUTA,*,# Midori HIRAMATSU, Hiroaki OHYA-NISHIGUCHI, Hitoshi KAMADA, and Kanae FUJII†
Institute for Life Support Technology, Yamagata Technopolis Foundation, 683 Kurumanomae, Numagi, Yamagata 990
†ESR Group, Research and Development Department, Analytical Instruments Division, JEOL Ltd., Akishima, Tokyo 196
(Received July 5, 1993)

The superoxide dismutase (SOD) activity of Cu,Zn-, Mn-, and Fe-SODs, and the SOD-*like* activity of ferricytochrome *c*, nitro blue tetrazolium (NBT), epinephrine, pyrogallol, L-ascorbic acid, and hydroxylamine, were investigated by the method of kinetic competition against superoxide radicals ($O_2^{-\cdot}$) using ESR spectroscopy with a nitrone spin-trap 5,5-dimethyl-1-pyrroline *N*-oxide (DMPO). These activities depended on the pH and/or kind of the $O_2^{-\cdot}$ generating system used. A comparison of the results obtained for two $O_2^{-\cdot}$ generating systems of KO_2 and hypoxanthine–xanthine oxidase showed that the effective pH in the former system was 1 or more higher than that in the latter. A new competition kinetic theory which includes a parameter of the stoichiometric ratio has been developed. Consequently, the profile of the non-stoichiometric competition reaction between DMPO and scavengers for $O_2^{-\cdot}$ was theoretically clarified.

Superoxide dismutase (SOD) plays an important role in defending a living body from oxidative stress by removing superoxide radicals ($O_2^{-\cdot}$).[1—5] A number of materials in addition to the SOD can also react to remove $O_2^{-\cdot}$.[2—5] Such reactivity of materials is often called an "SOD-*like* activity". Superoxide generation and the SOD-*like* activity have conventionally been measured by spectrophotometry,[1,6—10] while these are also measurable for ESR spectroscopy by applying a spin-trapping technique.[11,12] Recently, the ESR method is becoming extensively popular in chemical, biological, and medical fields because of: (1) the high specificity to $O_2^{-\cdot}$ and (2) no obstruction caused by the color and turbidity of samples.[13—26]

The ESR method consists of three constituents: (1) 5,5-dimethyl-1-pyrroline *N*-oxide (DMPO) as a spin-trap, (2) a test compound as a scavenger, and (3) a superoxide generating system as a radical source. Especially, the selection of the superoxide generating system is one of the most important keys to obtain accurate experimental results, because the reproducibility of the $O_2^{-\cdot}$ generation is directly related to the accuracy of the experiments. Many researchers prefer a stable hypoxanthine–xanthine oxidase (HPX–XOD) system,[11—14,16—22,24,25] whereas some researchers recommend a chemically pure potassium superoxide (KO_2) system rather than the HPX–XOD system.[14,15,23]

In our early work we formulated a method for calculating the second-order rate constant for the reaction between $O_2^{-\cdot}$ and scavengers to apply the ESR spin-trapping method, and found that the rate constants of Cu,Zn-SOD, Mn-SOD, Fe-SOD, celuroplasmin, ferricytochrome *c*, peroxidase, catalase, and L-ascorbic acid evaluated in the HPX–XOD system agreed with the literature values at pH 7.8.[22]

#Permanent address: ESR Group, Research and Development Department, Analytical Instruments Division, JEOL Ltd.

Recently, Gray and Carmichael used a similar ESR spin-trapping method with a dimethyl sulfoxide (DMSO) solution of KO_2 as an $O_2^{-\cdot}$ source, and reported that the rate constant for the reaction between Cu,Zn-SOD and $O_2^{-\cdot}$ was one order of magnitude larger than those for Mn- and Fe-SODs. They also described that an unusual dose response of SODs on scavenging $O_2^{-\cdot}$ could be explained from a Michaelis–Menten-*type* steady state kinetic model.[23]

Here, we try to reexamine these results through a comparison between both the KO_2 and HPX–XOD systems adopting several superoxide scavengers. Finally, we propose a kinetic model that has been newly improved so as to interpret the obtained results.

Experimental

Materials. A spin-trap, 5,5-dimethyl-1-pyrroline *N*-oxide (DMPO, Mitsui Toatsu Chemicals),[27] and a stable nitroxide radical, 4-hydroxy-2,2,6,6-tetramethylpiperidine-1-oxyl (TEMPOL, Sigma Chemical) were employed for a quantitative analysis of short-lived radicals. Potassium superoxide (KO_2, powder, Aldrich Chemical) in the presence of 1,4,7,10,13,16-hexaoxacyclooctadecane (18-crown-6 ether, a phase transfer catalyst, Aldrich Chemical) was adopted as a superoxide source. Milk xanthine oxidase (XOD, suspension, 20 unit/ml, Boehringer Mannheim) with hypoxanthine (HPX, Sigma Chemical) and diethylenetriamine-N,N,N',N'',N''-pentaacetic acid (DTPA, a metal ion chelator, Wako Pure Chemical) was used for another superoxide source. Several kinds of superoxide scavengers, such as cuprozinc superoxide dismutase (Cu,Zu-SOD, bovine erythrocyte, 3300 unit/mg protein, Boehringer Mannheim), mangano superoxide dismutase (Mn-SOD, *Escherichia coli*, 3840 unit/mg protein, Sigma Chemical), iron superoxide dismutase (Fe-SOD, *Escherichia coli*, 4900 unit/mg protein, Sigma Chemical), ferricytochrome *c* (horse heart, Sigma Chemical), nitro blue tetrazolium (NBT, Wako Pure Chemical), pyrogallol (Wako Pure Chemical), epinephrine (alias adrenalin, Wako Pure Chemical), L-ascorbic acid (Daiichi Pure Chemicals), and hydroxylamine hydrochloride ($NH_2OH{\cdot}HCl$, Wako Pure Chemical) were examined as received. The other chemicals

were of the highest grade commercially available.

Instruments. ESR spectra were recorded on a JEOL JES-RE1X spectrometer using a quartz flat cell (an ESR cuvette, type ES-LC12, inner size 60 mm×10 mm×0.3 mm). The obtained spectra were analyzed by a JEOL ESPRIT-385 on-line data system. The optical absorption spectra were measured using a Hitachi U-2000 spectrophotometer.

Preparation of Scavenger Solutions. Solutions of Cu,Zn-SOD (**1A**), Mn-SOD (**1B**), Fe-SOD (**1C**), ferricytochrome *c* (**1D**), NBT (**1E**), and NH_2OH·HCl (**1F**) were prepared by using distilled water. The pH unit of the concentrated solution of **1F** was adjusted to 7.8 or 6.2 by adding an adequate amount of NaOH. The precipitated NaCl was removed by filtration before use. Solutions of pyrogallol (**1G**), epinephrine (**1H**), and L-ascorbic acid (**1I**) were prepared by using ice-cold water containing 2 molar equivalents of HCl. To maintain the quality of the reagents, solutions of **1A**, **1B**, **1C**, **1D**, **1G**, **1H**, and **1I** were preserved on crushed ice during the experiments.

Preparation of Potassium Superoxide System. One hundred μmol (7.1 mg) of potassium superoxide (KO_2) was suspended in 1000 μl of dry DMSO containing 20% excess of 18-crown-6 ether (120 μmol, 31.7 mg) under dry argon atmosphere, and stirred for a few minutes. After waiting for a few minutes and removing any insoluble particles, 100 μl of a clear solution containing ca. 60 mM (1 M=1 mol dm^{-3}) KO_2 was put into a flask and diluted with 900 μl of dry DMSO. The freshly diluted solution (**2A**) contained 5—6 mM superoxide anion ($O_2^{-\cdot}$). Since **2A** was hygroscopic and then unstable for moisture, it was preserved in a silica-gel desiccator so as to avoid any absorbing moisture during the experiments. The half life of the $O_2^{-\cdot}$ observed in **2A** was of the order of 1 h under this condition, so that the ESR measurements were completed within 1/2 h after dilution.

The mixing procedure was as follows: One hundred μl of 200 mM sodium phosphate buffer solution (pH 7.8), 100 μl of a scavenger solution (**1A**—**1I**) (or water alone), and 15 μl of DMPO were mixed in a test tube.[28] Ten μl of **2A** was added to the mixed solution while vigorously stirring. To obtain good reproducibility of the adduct formation, the tip of the microsyringe quickly infusing **2A** was renewed each time. The mixture contained 0.22—0.27 mM KO_2, 0.53 mM 18-crown-6 ether, 4.4% volume of DMSO, 0.60 M DMPO, and an adequate amount of the scavenger in an 89 mM phosphate buffer solution at pH 7.8. This mixture was transferred into a flat cell. The signal intensity of the superoxide adduct (DMPO–O_2^-) after 30 s after mixing was measured.

Preparation of Hypoxanthine–Xanthine Oxidase System. Solutions of 2.0 mM HPX (**3A**), 5.5 mM DTPA (**3B**), and 0.33 unit/ml XOD (**3C**) were prepared by using a 133 mM sodium phosphate buffer solution at pH 7.8 or 6.2. To keep the activity of the XOD, the solution of **3C** was preserved on crushed ice during the experiments.

The mixing procedure was as follows: Fifty μl of **3A**, 35 μl of **3B**, 50 μl of a scavenger solution (**1A**—**1I**) (or water alone), and 15 μl of DMPO were mixed in a test tube.[28] Fifty μl of **3C** was added to the mixed solution, and stirred for several seconds. The mixture contained 0.50 mM HPX, 0.96 mM DTPA, 0.083 unit/ml XOD, 0.67 M DMPO, and an adequate amount of the scavenger in a 90 mM phosphate buffer solution at pH 7.8 or 6.2. This mixture was transferred into a flat cell. The signal intensity of the superoxide adduct (DMPO–O_2^-) after 85 s after mixing was measured.

Measurements. Superoxide generation was confirmed optically by the reduction of ferricytochrome *c* using its absorbance change at 550 nm.[1] The enzyme activity of Cu, Zn-, Mn-, and Fe-SODs was calibrated by the method of McCord and Fridovich.[1] The concentration of KO_2 in DMSO was estimated by ESR spectroscopy at liquid-nitrogen temperature (77 K). The superoxide adduct (DMPO–O_2^-) in aqueous solution was detected by ESR spectroscopy at room temperature (296 K), and the signal intensity of the lowest (or highest) field peak of the adduct was estimated to be a relative height against the signal intensity of manganese ion (Mn^{2+}) doped in MgO used as a secondary standard.[22] The absolute concentration of DMPO–O_2^- was determined by a double integration of the ESR spectrum. One μM TEMPOL aqueous solution was used as a primary standard of the double-integrated ESR absorption.

Results and Discussion

Potassium Superoxide System. When a DMSO solution of KO_2 was mixed with an aqueous solution of DMPO at pH 7.8, the superoxide adduct of DMPO (DMPO–O_2^-) was formed. Figure 1 shows the time-dependent ESR spectra in the KO_2 system. Nearly pure signals observed at 11 s (ca. 93%, see simulation) were assigned to typical superoxide adduct based on its ESR parameters (a_N=1.40 mT, $a_{H\beta}$=1.13 mT, $a_{H\gamma}$=0.125 mT, g_0=2.0058).[29] This adduct decreased spontaneously as a function of time. Within a few minutes, two secondary products, hydroxyl adduct (DMPO–OH, a_N=1.49 mT, $a_{H\beta}$=1.43 mT, g_0=2.0057)[29] and methyl adduct (DMPO–CH_3, a_N=1.62 mT, $a_{H\beta}$=2.32 mT, g_0=2.0055),[29] were grown markedly. These adducts were derivations from $O_2^{-\cdot}$, H_2O_2 (a dismutated product of $O_2^{-\cdot}$), DMPO, and DMSO.[13,30] According to the simulated spectrum at 178 s after mixing, the relative concentration of DMPO–O_2^- decreased to ca. 43%, and those of DMPO–OH and DMPO–CH_3, which overlapped with each other, concomitantly increased to ca. 40% and ca. 17%, respectively. At this time, the spectrum became no longer suitable for the selective quantification of the DMPO–O_2^-.

Figure 2 shows a semi-logarithmic plot for the time courses of the DMPO–O_2^-. To clarify the characteristic of the KO_2 system, the time course of DMPO–O_2^- in a HPX–XOD system at the same pH is duplicated on the figure. A typical J-curve observed in the HPX–XOD system suggests the behavior of the DMPO–O_2^- as being an intermediate product of the following consecutive reaction:[30,31]

$$O_2^{-\cdot} + \mathrm{DMPO} \xrightarrow{k_{\mathrm{DMPO}}} \underset{\text{(ESR-detectable)}}{\mathrm{DMPO\text{–}O_2^-}} \xrightarrow{k_d} \underset{\text{(ESR-silent)}}{\text{nonradical(s)}}, \quad (1)$$

which is induced by the consumption of dissolved oxygen and HPX in the ESR cuvette. A similar observation was made previously in neutrophil suspensions during a respiratory burst.[32] On the other hand, a linear rela-

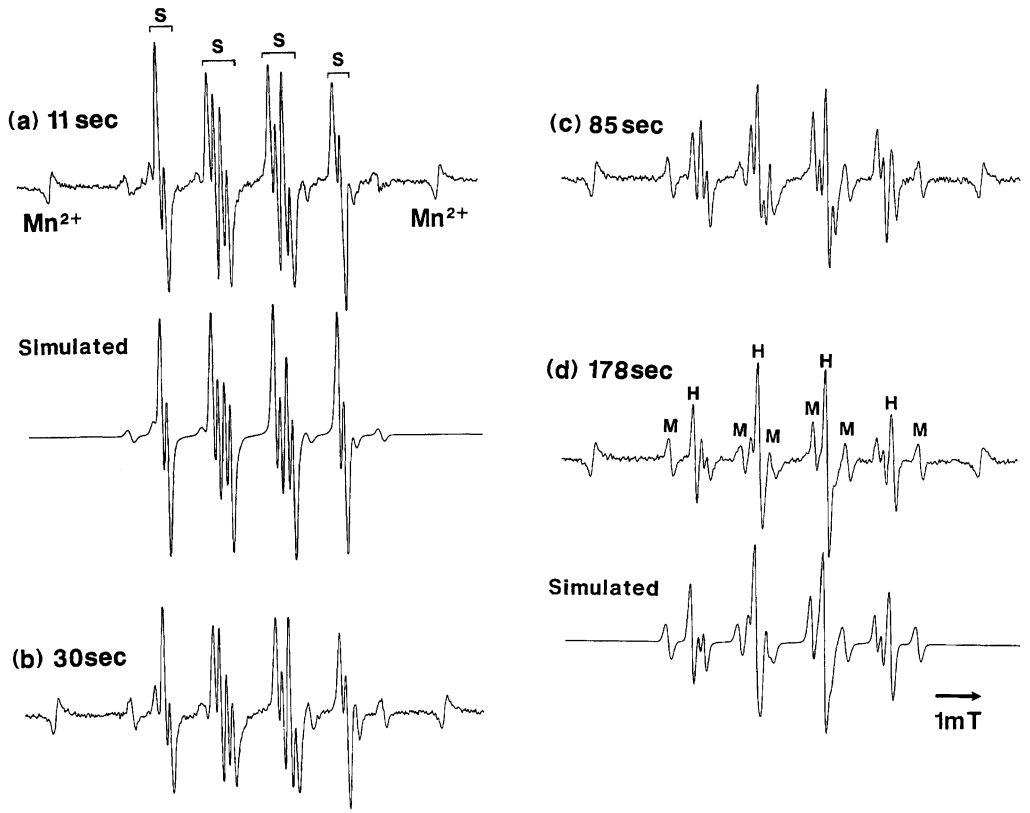

Fig. 1. Time-dependent ESR of DMPO spin adducts formed from the KO_2 system. The time after mixing is given above each spectrum. The spectra comprise three species: superoxide adduct (**S**), hydroxyl adduct (**H**), and methyl adduct (**M**). The medium contains 0.53 mM 18-crown-6 ether, 0.60 M DMPO, 4.4% DMSO, and 89 mM sodium phosphate (pH 7.8). Modulation amplitude was 0.05 mT (100 kHz), scan range 10 mT, scan time 5 s, response time 1 ms, microwave power 8 mW (9.414 GHz), accumulation count 8. The spectra observed at 11 s and 178 s were simulated as a mixture of three components: DMPO–O_2^- (ΔH_{msl}=0.10 mT, 50% Gaussian-50% Lorentzian shape), DMPO–OH (ΔH_{msl}=0.12 mT, 100% Gaussian shape), and DMPO–CH_3 (ΔH_{msl}=0.14 mT, 100% Gaussian shape). Simulated spectrum of (a) was composed of 93.1% DMPO–O_2^-, 3.7% DMPO–OH, and 3.2% DMPO–CH_3; simulated spectrum of (d) was composed of 42.5% DMPO–O_2^-, 40.3% DMPO–OH, and 17.2% DMPO–CH_3. The other ESR parameters are described in the text.

tionship between the log concentration of DMPO–O_2^- and the reaction time in the KO_2 system shows that the spontaneous decay of the DMPO–O_2^- follows a simple first-order kinetics with a rate constant of ca. 1.1×10^{-2} s^{-1}, the half life being ca. 60 s. This is close to the reported values at the physiological pH,[30,31] suggesting that the decay rate of the DMPO–O_2^- is almost independent of the kind of $O_2^{-\cdot}$ generating system when the pH condition is set so as to be similar. From the intercept of the straight line, the initial concentration of DMPO–O_2^- is estimated to be 2.6×10^{-5} M in the KO_2 system, yield 10—12% against KO_2.

Comparison of SOD-*like* Behaviors Observed in Two Kinds of the $O_2^{-\cdot}$ Generating Systems. When a known amount of a scavenger (Cu,Zn-SOD, Mn-SOD, Fe-SOD, ferricytochrome *c*, NBT, epinephrine, pyrogallol, L-ascorbic acid, and NH_2OH) was added to the above-mentioned systems, the intensity of the DMPO–O_2^- markedly decreased.[33] Since the half lives of the DMPO–O_2^- in the absence and presence of the scavengers were almost the same across a wide concentration range of the scavengers, such decreases are hardly due to an accerelation of the adduct decomposition. This indicates that: (1) the reactions of DMPO–O_2^- with the scavengers can be ignored under these conditions, and (2) the decrease in the signal intensities is mainly due to an inhibitory effect on the formation of the DMPO–O_2^- adduct.

Figure 3 shows the inhibitory effect of the scavengers. The results obtained at the same pH are considerably different between the two systems: The effect in the KO_2 system is summarized as Fe-SOD > Cu,Zn-SOD > Mn-SOD > pyrogallol > epinephrine > L-ascorbic acid ≈ NBT > ferricytochrome $c \gg NH_2OH$ (Fig. 3a), while that in the HPX–XOD system is summarized as SODs ≫ pyrogallol > L-ascorbic acid ≈ ferricytochrome *c* > epinephrine > NBT ≫ NH_2OH (Fig. 3b). This difference is discussed below based on a kinetic analysis.

Apparent Second-Order Rate Constant. To clarify the difference between the two systems, the apparent second-order rate constants for the reaction of the scavengers with $O_2^{-\cdot}$ (k_S's) were evaluated from the

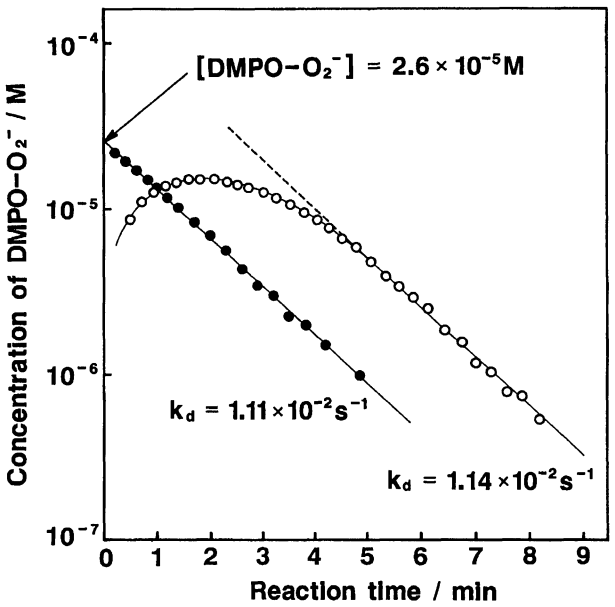

Fig. 2. Time course of the concentration of DMPO–O_2^- in both KO_2 (●) and HPX–XOD (○) systems at pH 7.8, 23 °C.

50% inhibitory doses (ID_{50}'s) by the method of Mitsuta et al:[22]

$$k_S = k_{DMPO} \cdot \frac{[DMPO]}{ID_{50}}, \quad (2)$$

where the ID_{50}'s observed in the HPX–XOD system at pH 6.2 (Fig. 3c) were adopted as being helpful for understanding the above-mentioned difference. The rate constants for the reaction of DMPO with $O_2^{-\cdot}$ at various pH (strictly speaking, with the mixture of $O_2^{-\cdot}/HO_2\cdot$) were calculated from the equation of Finkelstein et al:[12]

$$k_{DMPO} = \frac{k_{HO_2\cdot} + 10^{(pH-pK_a)} \cdot k_{O_2^-}}{1 + 10^{(pH-pK_a)}}, \quad (3)$$

where the constants, $k_{HO_2\cdot}$, $k_{O_2^-}$, and pK_a, are 6.6×10^3 $M^{-1}s^{-1}$, 10 $M^{-1}s^{-1}$, and 4.88, respectively.[12] We obtained the k_{DMPO}'s at pH 7.8 and 6.2 to be 18 $M^{-1}s^{-1}$ and 3.1×10^2 $M^{-1}s^{-1}$, respectively.[34] These values were used as a primary standard of all evaluations.

Table 1 lists the evaluated values of ID_{50} and k_S. When the pH was elevated from 6.2 to 7.8 in the HPX–XOD system, the k_S values for pyrogallol, epinephrine, and NBT increased (type A), while those for ferricytochcome *c*, L-ascorbic acid, and NH_2OH decreased (type B). On the other hand, at the same pH of 7.8, the k_S's for the scavengers of type A in the KO_2 system were larger than those in the HPX–XOD system. On the contrary, the k_S's for the scavengers of type B in the KO_2 system were smaller than those in the HPX–XOD system.

This observation suggests that the effective pH in the KO_2 system was 1 or more higher than that in the HPX–XOD system.[43] However, since two pH values before and after mixing of KO_2 coincide with each other within the experimental errors, the result cannot be ascribed to a pH change of the entire KO_2 system. We suppose that the alkaline shift of k_S specific to the KO_2 system is related to be the concentration gradient of KO_2 (or a pH gradient by KO_2) in the early stage of mixing, because (1) a KO_2 solution is a strong alkaline reagent and (2) KO_2 is so unstable for moisture that the $O_2^{-\cdot}$ generation from KO_2 and the reaction of $O_2^{-\cdot}$ with the scavengers is completed before the KO_2 solution diffuses to water uniformly. If this explanation is reasonable, the reason why the SOD activities become lower in the KO_2 system, rather than in the HPX–XOD system, can be explained by the same reason, namely, the SOD activities (especially of Mn- and Fe-SODs) decrease with increasing alkalinity.[37,44–48]

Time-Dependent Behavior of Inhibitory Effect in Potassium Superoxide System. In the KO_2 system, a difference in the time lag between dissolving KO_2 and measuring the ESR could not be ignored. For example, the use of a freshly prepared solution of KO_2 gave a steeply sloping inhibition curve for Cu,Zn-SOD with a large ID_{50}. However, when the KO_2 solution was kept in a silica-gel desiccator for 1/2 h, the profile of the curve changed to a gentle slope with a small ID_{50}. A similar changeability was widely observed in measuring the SOD-*like* activity using our KO_2 system. Because such a sensitive time-dependent behavior was not seen in the HPX–XOD system, this is a phenomenon that is specific to the KO_2 system and is nonspecific to the kind of scavengers. This fact suggests that: (1) a change in the quality of the KO_2 solution occurs as time passes, and (2) it is quite important for this system to be standardized by the time period after dissolving KO_2 in DMSO.

There is a considerable difference in the k_S values of the SODs between those evaluated in our KO_2 system (Table 1) and those reported by Gray and Carmichael ($k_{Cu,Zn\text{-}SOD}=6.4\times10^9$ $M^{-1}s^{-1}$, $k_{Mn\text{-}SOD}=6.8\times10^8$ $M^{-1}s^{-1}$, and $k_{Fe\text{-}SOD}=6.6\times10^8$ $M^{-1}s^{-1}$).[23] This indeterminable problem may be partly ascribable to such a difference in the time lag after preparing the KO_2 solution.

Theoretical Profile of Non-Stoichiometric Competition Reaction between DMPO and Scavengers for $O_2^{-\cdot}$. (i) Slope Variation of Sigmoidal-Shaped Inhibition Curves. In an earlier report, we theoretically explained the sigmoidal shape of inhibition curves by using a simple second-order reaction model.[22] However, there has still been an unexplained deviation in the observed curves from the theoretical one: A variation in the slopes which depends on the kind of scavengers and/or the experimental conditions (see Fig. 3). Recently, Gray and Carmichael described from the viewpoint of enzyme kinetics that the slope varied according to a difference in the overall reaction order of the dismutase enzymes.[23] However, such variations are widely observed not only in the enzyme systems, but also in a variety of systems, scavenging

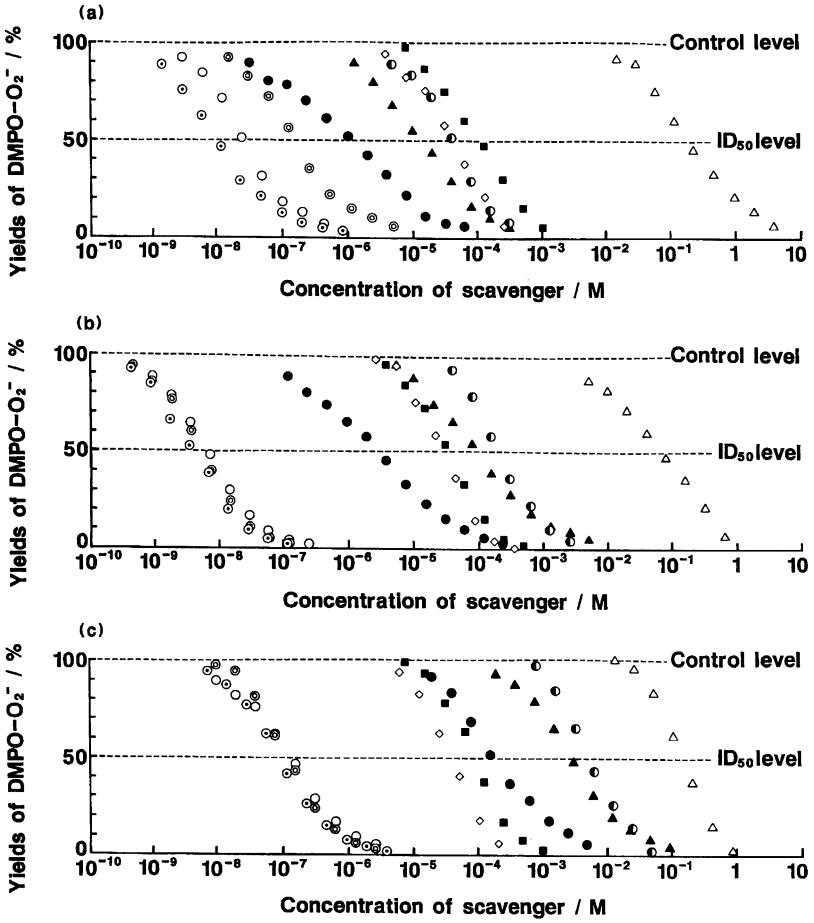

Fig. 3. Inhibitory effect of various superoxide scavengers on the formation of DMPO–O_2^- in (a) the KO_2 system at pH 7.8, (b) the HPX–XOD system at pH 7.8, and (c) the HPX–XOD system at pH 6.2, 23 °C. Simbols used are: Cu,Zn-SOD (○), Mn-SOD (◎), Fe-SOD (⊙), ferricytochrome *c* (■), NBT (◐), epinephrine (▲), pyrogallol (●), L-ascorbic acid (◇), and hydroxylamine (△).

radicals such as of H· and HO·.[49] We considered that this variation might more generally reflect a difference in the stoichiometric ratio between the reactants, rather than a difference in the reaction order, itself.[50] Here, we generalize the earlier explanation to the sigmoidal curves, as in the following:

$$O_2^{-\cdot} + \mathrm{DMPO} \xrightarrow{k_{\mathrm{DMPO}}} \mathrm{DMPO\text{–}O_2^-} \tag{4}$$

and

$$mO_2^{-\cdot} + n\mathrm{S} \xrightarrow{k_S^*} (\mathrm{S}_n\mathrm{O}_{2m})^{m-}, \tag{5}$$

where k_{DMPO} and k_S^* are rate constants, m and n are the molecule numbers, S and $(\mathrm{S}_n\mathrm{O}_{2m})^{m-}$ represent a scavenger molecule and a berthollide-*type* intermediate product, and the reaction orders of Eqs. 4 and 5 correspond to the second- and $(m+n)$th-order, respectively. These reactions constitute a couple of competitive reactions for $O_2^{-\cdot}$. If n molecules of the S (so-called "subunit") combine to form a highly functionalized oligomer (S_n) in the solution, this scheme will belong to a category of the typical enzyme kinetics. However, since in our case, most of the scavengers that we used were not enzymes, the S is assumed to dissolve solely in the solvent. Then, the initial velocities of two reactions are defined as

$$\frac{\mathrm{d[DMPO\text{–}O_2^-]}}{\mathrm{d}t} = k_{\mathrm{DMPO}}\cdot[\mathrm{DMPO}]\cdot[O_2^{-\cdot}] \tag{6}$$

and

$$\frac{\mathrm{d}[(\mathrm{S}_n\mathrm{O}_{2m})^{m-}]}{\mathrm{d}t} = k_S^*\cdot[\mathrm{S}]^n\cdot[O_2^{-\cdot}]^m, \tag{7}$$

where the total concentration of $O_2^{-\cdot}$ is a constant specific to the $O_2^{-\cdot}$ generating system. When a considerable portion X $(0<X<1)$ of the total $O_2^{-\cdot}$ is scavenged by S, the remaining $O_2^{-\cdot}$ which can react with DMPO reduces to $1-X$. Because $\mathrm{d[DMPO\text{–}O_2^-]}/\mathrm{d}t$ and $\mathrm{d}[(\mathrm{S}_n\mathrm{O}_{2m})^{m-}]/\mathrm{d}t$ are proportional to the order of $[O_2^{-\cdot}]$, the velocity ratio of the $O_2^{-\cdot}$ consumption caused by the Eqs. 4 and 5 is written as $(1-X):X^m$ obeying a simple mass law. In addition, according to Eqs. 4 and 5, one mole of $O_2^{-\cdot}$ consumption produces one mole of DMPO–O_2^- or $1/m$ mole of $(\mathrm{S}_n\mathrm{O}_{2m})^{m-}$. Therefore, the velocity ratio of the product formation is finally expressed as

$$\frac{\mathrm{d[DMPO\text{–}O_2^-]}}{\mathrm{d}t} : \frac{\mathrm{d}[(\mathrm{S}_n\mathrm{O}_{2m})^{m-}]}{\mathrm{d}t} = (1-X) : \frac{1}{m}\cdot X^m. \tag{8}$$

From Eqs. 6, 7, and 8, we can obtain formulae describing

Table 1. ID_{50}'s and Rate Constants of Several Superoxide Scavengers Evaluated by the Method of Second-Order Approximation

Substance	ID_{50}/M			$k_S/M^{-1}s^{-1}$			$k_{ref}/M^{-1}s^{-1}$	pH_{ref}	Method[c]	Ref.
	HPX–XOD (pH 6.2)	HPX–XOD (pH 7.8)	KO_2 (pH 7.8)	HPX–XOD (pH 6.2)	HPX–XOD (pH 7.8)	KO_2 [b] (pH 7.8)				
DMPO	—	—	—	—	—	—	3.1×10^2	6.2	②	12
							1.8×10^1	7.8		
Cu,Zn-SOD[a]	1.3×10^{-7} (13.7 U/ml)	7.5×10^{-9} (0.79 U/ml)	2.8×10^{-8} (2.96 U/ml)	1.6×10^9	1.6×10^9	3.9×10^8	ca.2×10^9	5—9.5	①	35,36
			1.2×10^{-8} [d] (1.27 U/ml)			9.0×10^8 [d]				
Mn-SOD[a]	1.2×10^{-7} (18.1 U/ml)	5.7×10^{-9} (0.87 U/ml)	1.6×10^{-7} (24.6 U/ml)	1.7×10^9	2.1×10^9	6.8×10^7	2.0×10^9	6.0	③	37,38
							1.8×10^9	7.8		
							3.3×10^8	10.2		
Fe-SOD[a]	8.8×10^{-8} (16.8 U/ml)	4.0×10^{-9} (0.76 U/ml)	1.1×10^{-8} (2.10 U/ml)	2.4×10^9	3.0×10^9	9.8×10^8	1.9×10^9	6.0	③	37,38
							1.6×10^9	7.8		
							3.8×10^8	10.2		
Ferricytochrome *c*	8.6×10^{-5}	2.7×10^{-5}	9.1×10^{-5}	2.4×10^6	4.5×10^5	1.2×10^5	1.4×10^6	4.7—6.7	①	39
							6.2×10^5	7.8		
							2.0×10^5	9.0		
							4.2×10^4	10.0		
NBT	5.0×10^{-3}	1.4×10^{-4}	4.3×10^{-5}	4.2×10^4	8.6×10^4	2.5×10^5	5.94×10^4	9.8	①	40
Epinephrine	2.6×10^{-3}	8.8×10^{-5}	1.2×10^{-5}	8.0×10^4	1.4×10^5	9.0×10^5	4×10^4	7.8	②	41
Pyrogallol	1.8×10^{-4}	2.8×10^{-6}	9.8×10^{-7}	1.2×10^6	4.3×10^6	1.1×10^7	—		④	This work
L-Ascorbic acid	3.6×10^{-5}	2.8×10^{-5}	4.0×10^{-5}	5.8×10^6	4.3×10^5	2.7×10^5	6.5×10^6	5.11	①	42
							5.2×10^6	5.27		
							8.9×10^5	6.2		
							3.6×10^5	6.71		
							2.7×10^5	7.4	②	9
							1.52×10^5	9.9	①	40
Hydroxylamine	1.4×10^{-1}	7.4×10^{-2}	2.0×10^{-1}	1.5×10^3	1.6×10^2	5.4×10^1	—		④	This work

a) The molarity of SOD was calculated from the activity unit (U/ml) of SOD at the 50% inhibition point, the specific activity of SOD (see Materials), and the molecular weights of SOD. The molecular weights used are: Cu,Zn-SOD (32000), Mn-SOD (40000), and Fe-SOD (39000). b) Rate constants of three kinds of SOD presented by Gray and Carmichael were retested in our KO_2 system. However, we could not obtain the similar results which they reported.[23] c) The methods used were: ① pulse radiolysis, ② competition with SOD, ③ competition with ferricytochrome *c*, and ④ competition with DMPO. d) Obtained after the KO_2 solution was kept for 30 min in a silica-gel desiccator.

k_S^* in the general and special ($X=0.5$) cases as

$$k_S^* = \frac{k_{DMPO}{}^m}{m}\cdot\frac{X^m}{(1-X)^m}\cdot\frac{[DMPO]^m}{[S]^n} \quad (9)$$

and

$$k_S^* = \frac{k_{DMPO}{}^m}{m}\cdot\frac{[DMPO]^m}{ID_{50}^n}, \quad (10)$$

respectively. Comparing the coefficients of Eqs. 9 and 10 leads us immediately to the following relationship:

$$[S]^n = \frac{X^m}{(1-X)^m}\cdot ID_{50}^n \quad (11)$$

or

$$[S] = \frac{X^f}{(1-X)^f}\cdot ID_{50}, \quad (12)$$

where a new factor f ($f=m/n$) is defined as an apparent molecule number of $O_2^{-\cdot}$ which one molecule of S can scavenge.

On the other hand, the signal intensity of DMPO–O_2^- during the early stage of the reaction is expressed as

$$I = (1-X)\cdot I_0, \quad (13)$$

where I_0 is the total amount of $[O_2^{-\cdot}]$ which can be trapped by DMPO in the absence of S, and I is the total amount of [DMPO–O_2^-] after spin adduct formation in the presence of S.

Variously sloping curves can be obtained from Eqs. 12 and 13 by changing X as a parameter combining I with [S]. Figure 4 shows the theoretically expected sigmoidal curves in which a marked slope variation occurred when the f value varied. As an example, we can duplicate the experimental data of pyrogallol observed in the HPX–XOD system at pH 7.8 on the figure. Thereby, the f value of pyrogallol is estimated to be an intermediate

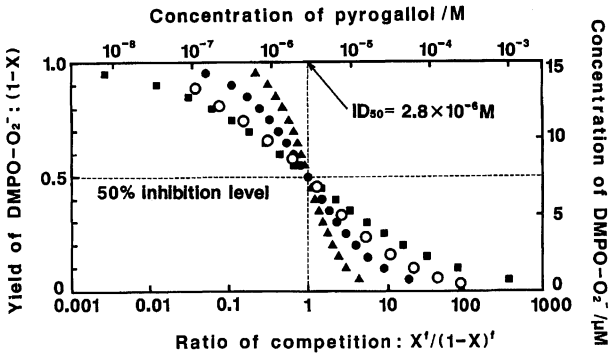

Fig. 4. Variation of the sigmoidal shapes on the inhibition curves: Theoretical values (▲: $f=0.5$, ●: $f=1$, ■: $f=2$), and experimental one of pyrogallol (○) shown in Fig. 3(b).

value between 1 and 2.

(ii) Influence of Slope Variation on Stern–Volmer-*type* Plot. When the experimental data, $(I_0/I)-1$, of Cu, Zn-SOD are plotted for the SOD concentration, the data arrangement shows good linearity.[9,51] Therefore, this Stern–Volmer-*type* plot, originally developed for analyzing fluorescence quenching,[52] is one of the most popular treatments for determining the unknown SOD activities of biological samples.[18] However, when all of the data, except for SOD, were treated on the plot, we often experienced a nonlinear data arrangement (usually a parabola-*like* curve). This phenomenon can be theoretically explained as an influence of the slope variation of sigmoidal curves. According to Eqs. 12 and 13, the relation between $(I_0/I)-1$ and [S] is expressed as

$$[S] = \{(I_0/I) - 1\}^f \cdot ID_{50}. \quad (14)$$

This equation indicates that: (1) the $(I_0/I)-1$ is proportional to $[S]^{1/f}$, and (2) the curvilinearity on the plot can be illustrated as an algebraic curve given by a monomial of degree $1/f$. Figure 5 shows a Stern–Volmer-*type* plot rearranged from Fig. 4. The data, except for $f=1$, surely shows a parabolic curvilinearity similar to that which we often experienced. This fact proves that such a curvilinearity is, partly at least, due to a reaction which depends on the f value.

(iii) Evaluating Method of f Value. When evaluating the f value, we can adopt the logarithmic form of Eq. 14:

$$\log[S] = f \cdot \log\{(I_0/I) - 1\} + \log ID_{50}, \quad (15)$$

where f and $\log ID_{50}$ mean a coefficient and an intercept, respectively. Equation 15 reveals that $\log[S]$ is a linear function to $\log\{(I_0/I)-1\}$ with a slope of f. We can evaluate the f value directly from the slope on the $\log\{(I_0/I)-1\}$ vs. $\log[S]$ plot.

This plot may be seen to be quite similar to that which Gray and Carmichael used,[23] though the meaning of the slope is theoretically different. If two or more molecules of the scavenger interact so as to react with two or more molecules of $O_2^{-\cdot}$, the slope will mean neither the actual reaction order of the scavenger nor that of $O_2^{-\cdot}$. It is a mere ratio of the stoichiometry between the two reactants, namely, $f(=m/n)$. Only when either m or n is known beforehand will we be able to determine the actual reaction orders.

Analysis of Experimentally Detected Slope Variation. (i) f Value. When we want to apply the theory of the f value to various scavengers we cannot avoid an important problem: The correction of the experimental errors caused by: (1) the reaction between DMPO–O_2^- and the scavengers (short-living of DMPO–O_2^-) and (2) the reaction between the scavengers and molecular oxygen (autoxidation). The former causes an intensity loss in DMPO–O_2^- during competition reactions; the latter causes a concentration loss in the scavengers before and during competition reactions. In our case, however, such a loss was hardly observed during a prelimitary examination across a wide range of inhibitions ($0<X<0.9$). Therefore, the correction becomes insignificant, and we can approximately analyze the sigmoidal curves of Fig. 3 without any correction (in the case of $X>0.9$, see next section).

Figure 6 shows a $\log\{(I_0/I)-1\}$ vs. $\log[S]$ plot for pyrogallol in the HPX–XOD system at pH 7.8, in which the data show a good linearity with a high correlation coefficient of 0.9986. From the slope of the straight line, the f value of pyrogallol is determined to be 1.47. The f value of the other scavengers and/or conditions can be determined in the same manner.

Table 2 lists the evaluated f values and their correlation coefficients r. In the HPX–XOD system, the f val-

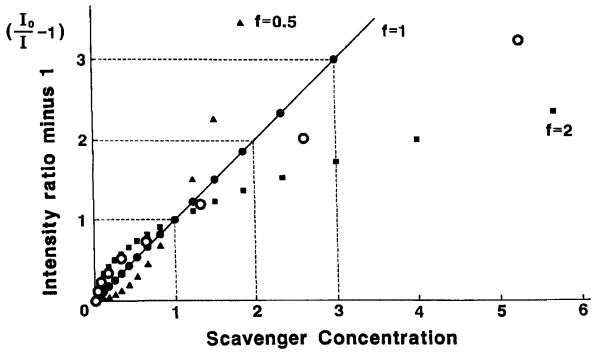

Fig. 5. Stern–Volmer-*type* plot for theoretical (▲: $f=0.5$, ●: $f=1$, ■: $f=2$) and experimental (○) data of Fig. 4. The concentration on the horizontal axis is a normalized value when ID_{50} is set to 1.

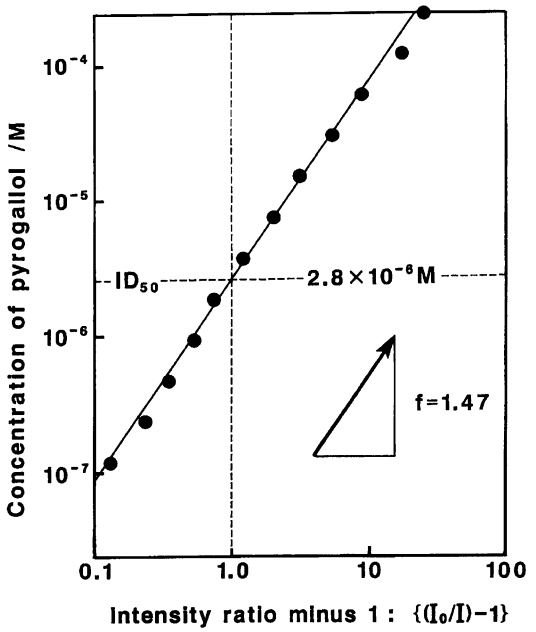

Fig. 6. Relation between $\log\{(I_0/I)-1\}$ and $\log[S]$ of pyrogallol observed in the HPX–XOD system at pH 7.8. The correlation coefficient r is 0.9986.

Table 2. Evaluated f Values and Correlation Coefficients r of Several Superoxide Scavengers

Substance	$f_{HPX-XOD}(r)$		$f_{KO_2}(r)$	f_{ref}	Ref.
	pH 6.2	pH 7.8	pH 7.8		
Cu,Zn-SOD	1.0_1 (0.999_6)	1.0_0 (0.999_0)	0.9_7 (0.994_7)	1.6_9[b]	23
			1.3_8 (0.987_2) [a]		
Mn-SOD	0.8_7 (0.999_4)	0.8_5 (0.997_5)	0.9_2 (0.984_9)	2.2_7[b]	23
Fe-SOD	0.9_4 (0.996_8)	0.9_3 (0.998_9)	1.1_6 (0.985_1)	2.0_8[b]	23
Ferricytochrome c	0.6_9 (0.981_8)	0.6_9 (0.978_9)	0.9_7 (0.978_9)		
NBT	0.7_9 (0.945_0)	0.7_9 (0.995_7)	0.8_5 (0.998_3)		
Epinephrine	1.0_3 (0.996_5)	1.3_9 (0.994_6)	1.1_5 (0.997_6)		
Pyrogallol	1.2_1 (0.997_4)	1.4_7 (0.998_6)	1.6_6 (0.954_7)		
L-Ascorbid acid	0.6_4 (0.973_5)	0.6_0 (0.950_4)	0.8_6 (0.955_4)	2	42
Hydroxylamine	0.6_1 (0.927_9)	1.3_9 (0.974_5)	1.1_7 (0.995_8)		
Mean±S.D.	0.87±0.19	1.01±0.31	1.08±0.24		

a) Obtained after the KO_2 solution was kept for 30 min in a silica-gel desiccator. b) Calculated from the data of Ref. 23.

ues for SODs, ferricytochrome c, NBT, and L-ascorbic acid were independent of the pH under these conditions, though those for epinephrine, pyrogallol, and NH_2OH were dependent on the pH. On the other hand, almost all of the f values in the KO_2 system, except for those of epinephrine and NH_2OH, were slightly larger than those evaluated in the HPX–XOD system.

The f values of epinephrine and NH_2OH in the KO_2 system are located in the middle of two f values evaluated in the HPX–XOD system at pH 6.2 and 7.8. This result cannot be ascribed to a pH gradient by the KO_2 mentioned above. However, it may be explained based on the concentration gradient of DMSO during the early stage of mixing, since: (1) DMSO is an aprotic solvent, and (2) the hydrophobicity of DMSO promotes protonation of the molecules of epinephrine and NH_2OH. The role of the proton is important in the reaction with $O_2^{-}\cdot$. As a result, the reaction mechanism is influenced so as to shift the f value acidulously.

Judging from the means and standard deviations (S. D.) of the f values calculated for the individual system, the stoichiometry between $O_2^{-}\cdot$ and many scavengers is roughly 1 : 1, though some of the f values deviate from 1 depending on the kind of scavengers. The stoichiometric ratio of $O_2^{-}\cdot$ to ascorbate in a pulse radiolysis and a flash photolysis systems was reported to be 2 : 1.[42] However, our result is considerably different from this literature value.

(ii) Correlation Coefficient r. The correlation coefficients of ferricytochrome c and L-ascorbic acid in both the HPX–XOD and KO_2 systems, NH_2OH in the HPX–XOD system, NBT in the same system at pH 6.2, and pyrogallol in the KO_2 system, are lower than the others under the systematic conditions. In most cases, the cause of the low correlation is due to a deviation of the data above ca. 90% inhibition. The deviation in this region corresponds to a 1—5% intensity loss of the DMPO–O_2^{-} against I_0, suggesting that a small amount of the DMPO–O_2^{-} was additionally lost in the presence of the concentrated scavengers. Since the half life of the DMPO–O_2^{-} near to this range cannot be measured accurately because of the low signal-to-noise ratio, whether the decay of DMPO–O_2^{-} was accelerated or not, is indeterminable. However, there have been some reports describing the redox reactions of DMPO–O_2^{-} (or DMPO itself) with coexisting species, such as ascorbate,[53] iron complexes,[11,31] and iron ion,[54] so that such side-reactions may have contributed to the deterioration of the correlation in this inhibition range.

(iii) Analogy with Hill Plot. Figure 6 and the f value remind us of the Hill plot and Hill coefficient $\underline{n}$, respectively.[55,56] The concept of the Hill coefficient as being an index of the "sigmoidicity" of the reaction was first advocated by Hill to rationalize the oxygen absorption curve of blood.[57] Comparatively speaking, X (scavenging ratio; $0<X<1$), [S] (scavenger concentration), ID_{50} (50% inhibitory dose of scavenger, an index of the scavenging efficiency), and f (ratio of stoichiometry) correspond to Y (oxygenation ratio; $0<Y<1$), P (oxygen pressure), P_{50} (oxygen pressure at 50% oxygenation, an index of the affinity to molecular oxygen), and $\underline{n}$ (in this case, $1/\underline{n}$) of the haemoglobin oxygenation theory,[56] respectively.

If this analogy is appropriate, the f value will provide valuable information concerning: (1) the aggregation or polymerization of the scavengers as an analogy with Hill's model,[57,58] (2) an intramolecular consecutive reaction of scavengers with $O_2^{-}\cdot$ as an analogy with Adair's model,[56,59] and (3) the co-operativity (or allostericity) of the scavengers for $O_2^{-}\cdot$ as an analogy with the MWC model.[60]

We may find the DMPO–O_2^{-} decaying accelerately by a reaction with the scavengers. This effect would also overlap with the actual non-stoichiometric effect, indicating that the apparant f value may possibly give misleading information. Nevertheless, there is a sufficient probability of scavengers showing noncovalent interactions due to association, complexation, and/or solvation among scavengers and/or against free radicals. In this case, our kinetic model

becomes practicable for approaching the action of scavengers, as if the Hill coefficient was being used for interpreting the complicated enzymatic reactions.

We thank Dr. Kiyoko Yamamoto of the Institute of Chemical and Physical Research (Riken) for her critical reading and helpful discussion of this manuscript during seven months, and Dr. Ikuko Ueno of Institute of Medical Science, the University of Tokyo, for her valuable comments concerning this work. One of us (K.M.) is indebted to Mr. Kazuo Oikawa, Mr. Masaaki Aoyama, Mr. Hiroyuki Noda, Mr. Toshiyuki Sato, Dr. Koichi Fukui, and Dr. Tetsuhiko Yoshimura of our Institute for their giving the opportunity to use some experimental apparatuses.

Appendix.

If the non-stoichiometric behavior of the reaction between spin-trap (T) and radical (R·) cannot be ignored, the competition reactions are written according to

$$m_1\mathrm{R}\cdot + n_1\mathrm{T} \xrightarrow{k_{\mathrm{T}}^*} (\mathrm{T}_{n_1}\mathrm{R}_{m_1}) \tag{A1}$$

and

$$m_2\mathrm{R}\cdot + n_2\mathrm{S} \xrightarrow{k_{\mathrm{S}}^*} (\mathrm{S}_{n_2}\mathrm{R}_{m_2}). \tag{A2}$$

Then, the velocity of each reaction will be defined as

$$\frac{\mathrm{d}[(\mathrm{T}_{n_1}\mathrm{R}_{m_1})]}{\mathrm{d}t} = k_{\mathrm{T}}^*\cdot[\mathrm{T}]^{n_1}\cdot[\mathrm{R}\cdot]^{m_1} \tag{A3}$$

and

$$\frac{\mathrm{d}[(\mathrm{S}_{n_2}\mathrm{R}_{m_2})]}{\mathrm{d}t} = k_{\mathrm{S}}^*\cdot[\mathrm{S}]^{n_2}\cdot[\mathrm{R}\cdot]^{m_2}. \tag{A4}$$

According to a simple mass law, the velocity ratio can be expressed as

$$-\frac{\mathrm{d}[\mathrm{R}\cdot]}{\mathrm{d}t} : \frac{\mathrm{d}[(\mathrm{T}_{n_1}\mathrm{R}_{m_1})]}{\mathrm{d}t} : \frac{\mathrm{d}[(\mathrm{S}_{n_2}\mathrm{R}_{m_2})]}{\mathrm{d}t} = 1 : \frac{1}{m_1}\cdot(1-X)^{m_1} : \frac{1}{m_2}\cdot X^{m_2}. \tag{A5}$$

From Eqs. A3, A4, and A5, we can obtain the relationships:

$$I = \frac{1}{m_1}\cdot(1-X)^{m_1}\cdot I_0 \tag{A6}$$

and

$$[\mathrm{S}] = \{X/(1-X)\}^f\cdot \mathrm{ID}_{50}, \tag{A7}$$

where the expornent f is defined as m_2/n_2. These equations can be used as a mother tool for analyzing the competition reactions through the use of our spin-trapping method.

References

1) J. M. McCord and I. Fridovich, *J. Biol. Chem.*, **244**, 6049 (1969).
2) "Kassei Sanso (Active Oxygen)," ed by M. Nakano, K. Asada, and Y. Ōyanagui, *Tampakushitsu Kakusan Koso*, **33**, No. 16 (1988).
3) B. Halliwell and J. M. C. Gutteridge, "Free Radicals in Biology and Medicine," Clarendon Press, Oxford (1985), translated by M. Matsuo, M. Sagai, and T. Yoshikawa, Gakkai Shuppan Center, Tokyo (1988).
4) "Kassei Sanso (Active Oxygen)," ed by E. Niki and H. Shimasaki, Ishiyaku Shuppan, Tokyo (1987).
5) Y. Ōyanagui, "Superoxide To Igaku (Superoxide and Medicine)," Kyoritsu Shuppan, Tokyo (1981).
6) C. Beauchamp and I. Fridovich, *Anal. Biochem.*, **44**, 276 (1971).
7) H. P. Misra and I. Fridovich, *J. Biol. Chem.*, **247**, 3170 (1972).
8) S. Marklund and G. Marklund, *Eur. J. Biochem.*, **47**, 469 (1974).
9) M. Nishikimi, *Biochem. Biophys. Res. Commun.*, **63**, 463 (1975).
10) E. F. Elstner and A. Heupel, *Anal. Biochem.*, **70**, 616 (1976).
11) E. Finkelstein, G. M. Rosen, E. J. Rauckman, and J. Paxton, *Mol. Pharmacol.*, **16**, 676 (1979).
12) E. Finkelstein, G. M. Rosen, and E. J. Rauckman, *J. Am. Chem. Soc.*, **102**, 4994 (1980).
13) I. Ueno, M. Kohno, K. Yoshihira, and I. Hirono, *J. Pharm. Dyn.*, **7**, 563 (1984).
14) I. Ueno, M. Kohno, K. Haraikawa, and I. Hirono, *J. Pharm. Dyn.*, **7**, 798 (1984).
15) W. Korytowski, B. Kalyanaraman, I. A. Menon, T. Sarna, and R. C. Sealy, *Biochim. Biophys. Acta*, **882**, 145 (1986).
16) M. Hiramatsu and M. Kohno, *JEOL News*, **23A**, 7 (1987).
17) S. Uchida, R. Edamatsu, M. Hiramatsu, A. Mori, G. Nonaka, I. Nishioka, M. Niwa, and M. Ozaki, *Med. Sci. Res.*, **15**, 831 (1987).
18) H. Miyagawa, T. Yoshikawa, T. Tanigawa, N. Yoshida, S. Sugino, M. Kondo, H. Nishikawa, and M. Kohno, *J. Clin. Biochem. Nutr.*, **5**, 1 (1988).
19) T. Hatano, R. Edamatsu, M. Hiramatsu, A. Mori, Y. Fujita, T. Yasuhara, T. Yoshida, and T. Okuda, *Chem. Pharm. Bull.*, **37**, 2016 (1989).
20) M. Nukatsuka, H. Sakurai, and J. Kawada, *Biochem. Biophys. Res. Commun.*, **165**, 278 (1989).
21) R. Ogura, H. Ueta, M. Sugiyama, and T. Hidaka, *J. Invest. Dermatol.*, **94**, 227 (1990).
22) K. Mitsuta, Y. Mizuta, M. Kohno, M. Hiramatsu, and A. Mori, *Bull. Chem. Soc. Jpn.*, **63**, 187 (1990).
23) B. Gray and A. J. Carmichael. *Biochem. J.*, **281**, 795 (1992).
24) M. Hiramatsu, M. Kohno, R. Edamatsu, K. Mitsuta, and A. Mori, *J. Neurochem.*, **58**, 1160 (1992).
25) K. Takagi, H. Kanemitsu, N. Tomukai, H. Oka, A. Tamura, M. Kohno, K. Mitsuda, S. Yoshida, and K. Sano, *Neurol. Res.*, **14**, 26 (1992).
26) H. Ohya-Nishiguchi, "SOD," in "Sozai No ESR Hyōka-hō (The ESR Methods of Evaluating Materials)," ed by H. Ohya-Nishiguchi and J. Yamauchi, IPC, Tokyo (1992), Chap. 5.3, p. 444.
27) This DMPO was a colorless, odorless solid, and had a melting point of 27—28 °C.
28) a) The concentration loss of the scavenger due to autoxidation was not observed within the period; b) In general, an aqueous solution of pyrogallol can absorb molecular oxygen at alkaline pH by inducing its autoxidation. However, this velocity of the autoxidation below pH 7.8 was very slow. A similar observation was reported previously (Ref. 8).
29) G. R. Buettner, *Free Rad. Biol. Med.*, **3**, 259 (1987).

30) P. Kuppusamy and J. L. Zweier, *J. Biol. Chem.*, **264**, 9880 (1989).
31) I. Yamazaki, L. H. Piette, and T. A. Grover, *J. Biol. Chem.*, **265**, 652 (1990).
32) I. Ueno, M. Kohno, K. Mitsuta, Y. Mizuta, and S. Kanegasaki, *J. Biochem.* (*Tokyo*), **105**, 905 (1989).
33) These results were partly presented at the "12th Annual Meeting of Japan Society of Magnetic Resonance for Life Science," Tokyo, May 11—12, 1990 (Presentation, May 12); K. Mitsuta, M. Kohno, Y. Mizuta, M. Yamada, and M. Aoyama, "Magnetic Resonance in Medicine, Vol. 2 (Zikikyōmei To Igaku 2)," ed by E. Niki, K. Kakinuma, and T. Yoshikawa, Nihon-Igakukan, Tokyo (1991), p. 190.
34) The rate constants reported by Finkelstein et al. (Ref. 12) still remain to be the only data across a wide range of pH, and our rate constant (18 $M^{-1} s^{-1}$ at pH 7.8) obtained from them is about tenfold larger than the latest value (1.2 $M^{-1} s^{-1}$ at pH 7.4, 25 °C) reported by Yamazaki et al. (Ref. 31). We consider that using the former values is the best choice because of a good fit to our experimental results.
35) D. Klug, J. Rabani, and I. Fridovich, *J. Biol. Chem.*, **247**, 4839 (1972).
36) G. Rotilio, R. C. Bray, and E. M. Fielden, *Biochim. Biophys. Acta*, **268**, 605 (1972).
37) H. J. Forman and I. Fridovich, *Arch. Biochem. Biophys.*, **158**, 396 (1973).
38) There is a number of variation about rate constant values of Mn- and Fe-SODs (Refs. 37, 44, 45, 46, and 47), and those reported by Forman and Fridovich (Ref. 37) showed a good fit to our experimental results.
39) J. Butler, G. G. Jayson, and A. J. Swallow, *Biochim. Biophys. Acta*, **408**, 215 (1975).
40) B. H. J. Bielski and H. W. Richter, *J. Am. Chem. Soc.*, **99**, 3019 (1977).
41) K. Asada and S. Kanematsu, *Agric. Biol. Chem.*, **40**, 1891 (1976).
42) D. E. Cabelli and B. H. J. Bielski, *J. Phys. Chem.*, **87**, 1809 (1983).
43) In general, the value of k_{DMPO} decreases with increasing alkalinity (Ref. 12). Therefore, if pH value is locally elevated over 7.8 in the KO_2 system, the effective k_{DMPO} must be assumed as being less than 18 $M^{-1} s^{-1}$; otherwise the k_S's will be overestimated as too large values (Ref. 23). In the KO_2 system, it may be suitable to use the value of k_{DMPO} being 10 $M^{-1} s^{-1}$ or less, rather than 18 $M^{-1} s^{-1}$, at pH 7.8.
44) M. Pick, J. Rabani, F. Yost, and I. Fridovich, *J. Am. Chem. Soc.*, **96**, 7329 (1974).
45) A. Terech, J. Pucheault, and C. Ferradini, *Biochem. Biophys. Res. Commun.*, **113**, 114 (1983).
46) F. Lavelle, M. E. McAdam, E. M. Fielden, P. B. Roberts, K. Puget, and A. M. Michelson, *Biochem. J.*, **161**, 3 (1977).
47) C. Bull and J. A. Fee, *J. Am. Chem. Soc.*, **107**, 3295 (1985).
48) According to Refs. 45 and 47, the cause of low activities on Mn- and Fe-SODs above pH 10 is mainly due to a marked increase of the Michaelis constant (K_M) of SODs against $O_2^{-\cdot}$.
49) K. Makino, M. M. Mossoba, and P. Riesz, *J. Phys. Chem.*, **87**, 1369 (1983).
50) This consideration was first presented at the "13th Annual Meeting of Japan Society of Magnetic Resonance for Life Science," Kurume, May 9—10, 1991 (Presentation, May 9); K. Mitsuta, Y. Mizuta, M. Kusai-Yamada, and M. Kohno, "Magnetic Resonance in Medicine, Vol. 3 (Zikikyōmei To Igaku 3)," ed by R. Ogura and T. Yoshikawa, Nihon-Igakukan, Tokyo (1992), p. 102.
51) Y. Sawada and I. Yamazaki, *Biochim. Biophys. Acta*, **327**, 257 (1973).
52) See, for instance: J. D. Morrisett, H. J. Pownall, and A. M. Gotto, Jr., *J. Biol. Chem.*, **250**, 2487 (1975).
53) J. R. Harbour and J. R. Bolton, *Biochem. Biophys. Res. Commun.*, **64**, 803 (1975).
54) K. Makino, T. Hagiwara, A. Hagi, M. Nishi, and A. Murakami, *Biochem. Biophys. Res. Commun.*, **172**, 1073 (1990).
55) A. Cornish-Bowden, "Principles of Enzyme Kinetics," Butterworths, London (1976), Chap. 7.3, p. 120.
56) a) K. Imai, *Seikagaku*, **54**, 197 (1982); b) K. Imai, "Allosteric Effects in Haemoglobin," Cambridge University Press, Cambridge (1982).
57) A. V. Hill, *J. Physiol.*, **40**, proc. iv (1910).
58) D. V. Roberts, "Enzyme Kinetics," Cambridge University Press, Cambridge (1977), Chap. 8.2.3, p. 200.
59) a) G. S. Adair, *J. Biol. Chem.*, **63**, 529 (1925); b) G. S. Adair, *Proc. R. Soc., Ser. A*, **109**, 292 (1925).
60) J. Monod, J. Wyman, and J.-P. Changeux, *J. Mol. Biol.*, **12**, 88 (1965).